STATISTICS OF ATMOSPHERIC TURBULENCE WITHIN AND ABOVE A CORN CANOPY

J. D. WILSON*, D. P. WARD**, G. W. THURTELL, and G. E. KIDD

Department of Land Resource Science, University of Guelph, Guelph, Ontario, Canada

(Received in final form 30 September, 1982)

Abstract. Two three-dimensional split-film anemometers were used to measure turbulence statistics within and above a corn canopy. Normalised profiles of mean windspeed, root-mean-square velocity, momentum flux, and heat flux were constructed from half-hourly averages by dividing within-canopy measurements by the simultaneous canopy-top measurement. With the exception of the heat flux, these profiles showed consistent shape from day to day. Time series of the three velocity components were recorded on magnetic tape and subsequently analysed to obtain Eulerian time and length scales and the power spectrum of each component at several heights. The timescale was found to have a local minimum value at the top of the canopy. However the length scale L_w formed from the timescale and the root-mean-square vertical velocity varied with height as $L_w \simeq 0.1\, z$. The power-spectra were non-dimensionalised to facilitate comparison of spectra at different heights and times. All spectra had $-5/3$ regions spanning at least two decades in frequency.

1. Introduction

A good understanding of turbulence statistics within and above a plant community is a prerequisite to understanding turbulent transport of water vapour, carbon dioxide, oxygen, disease spores, pollen and damaging pollutants within a crop. However, much work concerning transport in and above forests and agricultural crops has been carried out without any detailed knowledge of the statistics of the turbulence in these environments; the fluxes are assumed to be linearly related to the mean concentration gradients, with a spatially varying 'constant' of proportionality, the eddy diffusivity (K), presumed to be a function of the turbulence. It is widely recognised (Tennekes and Lumley, 1972; Corrsin, 1974) that this relationship is not realistic in systems in which the turbulence length scale is large compared with the distance over which the concentration gradient may change significantly. Forest and agricultural canopies are systems in which K-theory should be used only with great care.

The dependence of studies in the literature on K-theory is probably a consequence of lack of detailed data on canopy turbulence statistics, and this in turn is due to the technical difficulty of constructing an anemometer satisfying the requirements of broad-band frequency response, small sampling volume, and unambiguous response to winds from all directions within the total solid angle. To date, the only anemometers satisfying all of the above requirements are the servo-controlled split-film heat-transfer anemometer described by Shaw *et al.* (1973) and modified by Ward (1977), and the multiple-element hot-film anemometer described by Lang and Leuning (1981).

* Present affiliation: New Zealand Meteorological Service, P.O. Box 722, Wellington, New Zealand.
** Present affiliation: Micro Systems Engineering, Suite 303, 2130 Lawrence Ave East, Scarborough, Ontario, Canada M1R 3A6.

Boundary-Layer Meteorology **24** (1982) 495–519. 0006–8314/82/0244–0495$03.75.

Shaw *et al.* (1973) and Ward (1977) have compared velocity statistics measured with the split-film (SF) anemometer with simultaneous statistics obtained using cup, pressure-sphere, propellor, and sonic anemometers. Shaw *et al.* (1974a, b) have presented velocity statistics measured with the SF anemometers within and above plant and forest canopies. This paper presents turbulence data based on over 100 hr of measurements with the SF anemometers within and above a mature corn canopy. Vertical profiles of mean windspeed, cup windspeed, the standard deviations of the three velocity components, turbulence intensity, shear stress, and heat flux were obtained. Spectral analysis was performed on data collected within and above the canopy and estimates of the turbulence time and length scales were computed from the autocorrelation functions and velocity component variances. The intention of the work was to provide detailed statistics of the turbulence within a corn canopy for input to a Lagrangian model of turbulent dispersion based on numerical simulation of particle trajectories (Wilson *et al.*, 1981).

2. Site and Experimental Procedure

The measurements were made in a 25 ha cornfield at the Elora Research Station, Elora, Ontario, Canada, during the summers of 1976 and 1977. The field slope was less than 2% and the fetch never less than 200 m.

During the 1976 measurement period, September 13 to October 5, the height of the canopy was 225 cm. A sonic anemometer* was operated at a height $z = 370$ cm (all heights to be given were measured from the ground). A SF anemometer was operated at one of several heights (75, 125, 175, 225, 275, 370, 655 cm). Simultaneous time series of the velocity components (u, v, w) in directions (x, y, z) at the two heights were recorded on a Sangamo** model 3562 FM tape recorder for subsequent spectral analysis. A total of 30 hr of data were recorded, with at least two hours of split-film data at each height.

During the 1977 measurement period, July 28 to September 3, the distribution of the vegetative area with height was approximately constant. The average height to the top of the tassles, measured frequently using samples of 50 plants, increased from 212 to 227 cm during this time. There were 59 000 plants per hectare, and the leaf area index was 2.9. The three velocity components were measured at two heights using split film anemometers. Temperature fluctuations for heat flux calculations were measured using miniature fine wire resistance thermometers, which were attached to the anemometer probes within 2 cm of the velocity sensors and rotated with the probe so as never to lie upwind or downwind of the velocity sensors. The sensing volume thus defined was very small (diameter $\simeq$ 5 cm).

Signals from the sensors were sampled 100 times per second by a Honeywell H316 minicomputer which accumulated the means, variances and covariances and at the end

* Kaijo Denki Co. Ltd., Tokyo, Japan.

** Sangamo Electric Co., Springfield, Illinois, U.S.A.

TABLE I

Daily comparisons of anemometers 1 and 2 at $z = H$ during 1977. The numbers given are the mean ratio and, in brackets, the standard deviation of the sample of individual 1/2 hourly ratios for the given day.

Day/Mo.	28/7	30/7	31/7	2/8	4/8	11/8	12/8	13/8	23/8	24/8	26/8	28/8	3/9
$\bar{u}_1/\bar{u}_2$	0.993 (0.007)	0.998 (0.011)	0.977	1.021 (0.021)	0.974 (0.011)	1.005 (0.010)	0.980 (0.015)	1.004 (0.005)	1.014 (0.008)	0.968 (0.014)	1.012 (0.019)	1.028 (0.005)	1.001 (0.007)
s_1/s_2	1.001 (0.005)	1.007 (0.010)	0.970	1.023 (0.019)	0.990 (0.016)	1.019 (0.013)	1.005 (0.001)	1.013 (0.005)	1.024 (0.005)	0.983 (0.011)	1.020 (0.017)	1.030 (0.005)	1.007 (0.006)
$\sigma_{u_1}/\sigma_{u_2}$	1.006 (0.010)	1.014 (0.009)	0.941	1.008 (0.014)	0.962 (0.004)	0.985 (0.011)	0.980 (0.015)	0.991 (0.021)	0.992 (0.008)	0.982 (0.009)	0.986 (0.013)	1.007 (0.004)	0.983 (0.008)
$\sigma_{v_1}/\sigma_{v_2}$	1.000 (0.015)	1.029 (0.014)	0.965	1.009 (0.010)	0.990 (0.010)	1.022 (0.009)	0.996 (0.006)	1.019 (0.009)	1.026 (0.004)	1.002 (0.015)	1.022 (0.018)	1.020 (0.008)	1.009 (0.012)
$\sigma_{w_1}/\sigma_{w_2}$	1.065 (0.008)	1.060 (0.026)	0.994	1.022 (0.014)	1.002 (0.020)	1.037 (0.006)	1.002 (0.008)	1.021 (0.008)	0.993 (0.015)	0.972 (0.016)	0.986 (0.017)	1.027 (0.010)	0.973 (0.014)
$\sigma_{T_1}/\sigma_{T_2}$				1.078 (0.050)	1.027 (0.046)		1.013 (0.001)	1.000 (0.067)		1.067 (0.031)	0.996 (0.030)	1.032 (0.040)	1.012 (0.007)
τ_1/τ_2			0.942	1.047 (0.041)	0.990 (0.068)	1.027 (0.019)	0.874 (0.039)	0.934 (0.028)				1.021 (0.075)	
A_1/A_2				1.153 (0.150)	1.027 (0.089)		1.082 (0.030)	1.014 (0.060)		0.973 (0.024)	0.957 (0.064)	1.076 (0.032)	0.932 (0.050)
number of 1/2 hr comparisons	5	4	1	4	3	3	2	4	3	7	6	6	5

of each run (usually 1/2 hr) performed a coordinate transformation which made $\bar{v} = \bar{w} = 0$ independently at each anemometer (Tanner and Thurtell, 1969), and printed the results. Profiles of the turbulence statistics throughout the canopy were obtained by operating one anemometer-thermometer at the top of the canopy, and another within the canopy at a height which was changed from run to run, throughout the experiments covering the range from 9 to 220 cm. Approximately 90 hours of data were obtained.

The instruments were placed between rows, but it was necessary to break off parts of leaves to avoid destruction of the anemometers. Damage to the canopy was kept to a minimum and the site changed several times, so the data should closely represent a healthy, undamaged canopy.

At the beginning of each day's measurements in 1976 the sonic and split-film anemometers were compared for 1 hr at $z = 370$ cm. During 1977 the two split-film anemometers and thermometers were compared at the canopy top for several 1/2 hr runs. If the comparison was unsatisfactory, the anemometers were recalibrated. Table I shows results of the comparisons for those days of the 1977 season for which statistics will be presented.

The symbols used in Table I are:

$(\sigma_u, \sigma_v, \sigma_w)$, the standard deviations of (u, v, w)
$s = \sqrt{\overline{u^2} + \overline{v^2}}$, the 'cup' windspeed
σ_T, the standard deviation of the temperature fluctuations
A, the sensible heat flux density
τ, the momentum flux density
H, canopy height.
An overbar denotes a time average value.

The high accuracy of the SF anemometers is apparent from Table I. However, note that while the turbulence intensity at the top of the canopy (typically $\sigma_u/\bar{u} \approx 0.7$) is much greater than that in the wind tunnel used for calibrations, satisfactory performance at the top of the canopy does not guarantee adequate performance lower in the canopy, where $\sigma_u/\bar{u}$ may have a value as large as 5, and the timescale of the turbulence decreases. The limiting factor low in the canopy, assuming speeds large enough to guarantee forced convection from the heated film ($\gtrsim 20$ cm s^{-1}), is the inertia of the servo system used to control the instantaneous angle β between wind direction and probe orientation at sufficiently small values to allow accurate correction for along-film-axis flow. At 5 Hz the servo system angular displacement ratio was 0.5 (obtained by applying a known sine wave to the servosystem input and measuring the resulting amplitude of servomotor displacement). Measurements within the canopy indicated that 90% of the time $|\beta| < 30°$.

3. Data of 1977 – Vertical Profiles

The profiles to be presented are constructed from data from many different runs on different days, appropriately normalised. A lack of scatter indicates that the shape of

the normalised profile is invariant from day to day. Let a subscript H denote a value at canopy height.

3.1. Wind direction

The coordinate rotation set $\bar{v} = 0$ at each anemometer for each period. Inspection of the rotation angles $\tan^{-1}(\bar{v}/\bar{u})$ in principle allows correlation of the wind direction at two sites, but each time an anemometer was moved, an unknown offset was introduced in the azimuth angle with respect to the higher anemometer. The best that one can hope to achieve from the available data is to correlate changes in wind direction at two levels which occur during a series of several runs with the anemometers undisturbed.

In comparing indicated direction changes at canopy top and within the canopy, it is possible to find large well-correlated changes, and large poorly-correlated changes. We can say nothing definitive about the variation of mean wind direction with height in the canopy. Perhaps some of the scatter in the experimental data to be presented could be reduced by a classification according to wind direction with respect to the row orientation. However, during the experiments the impression was formed that the wind direction was not causing noticeable changes in the observed statistics. The appearance of this densely planted crop was not dramatically anisotropic (except of course near ground) and it seems unlikely that a fluid element passing along the row would encounter significantly less vegetation than one moving across the row. Certainly in future experiments wind direction should be recorded.

3.2. Means and standard deviations of wind velocities

Figures 1 and 2 show the normalised profiles of $\bar{u}$ and cup windspeed s, both of which are well behaved functions of height. The dashed lines are the curves:

$$\bar{u} = \bar{u}_{220} \exp\left(4.0\left(\frac{z}{220} - 1\right)\right)$$

$$s = s_{220} \exp\left(3.0\left(\frac{z}{220} - 1\right)\right).$$

No secondary maximum was observed in the wind profile near the bottom of the canopy, in contrast with the findings of Bill *et al.* (1976) but in agreement with most observations within dense, mature corn canopies. The profile of s/s_H versus z/H resembles that reported by Shaw *et al.* (1974b) for a crop of height $\simeq 280$ cm, and their comments regarding the inadequacy of the exponential wind profile near the canopy top, where $\partial^2 s/\partial z^2 < 0$, also apply here. See Seginer *et al.* (1976) for a demonstration that an exponential canopy wind profile would be expected on the assumption of a height independent Prandtl mixing length (defined by $l = \sqrt{\tau/p}/(\mathrm{d}\bar{u}/\mathrm{d}z)$ which implies $K = l^2\,\mathrm{d}\bar{u}/\mathrm{d}z$ where K is the eddy viscosity) and a vertically uniform canopy.

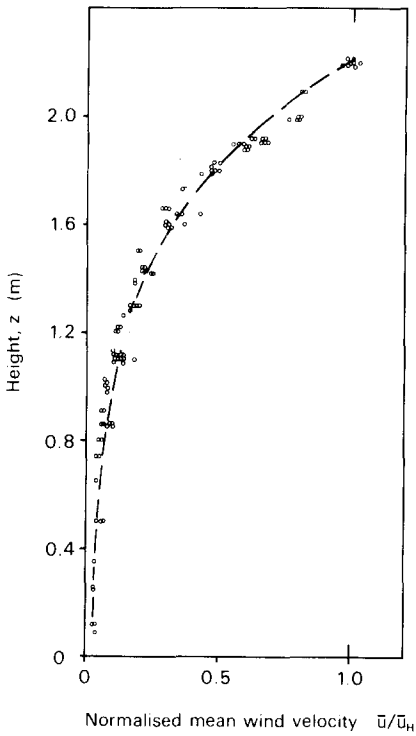

Fig. 1. Profile of normalised mean wind velocity.

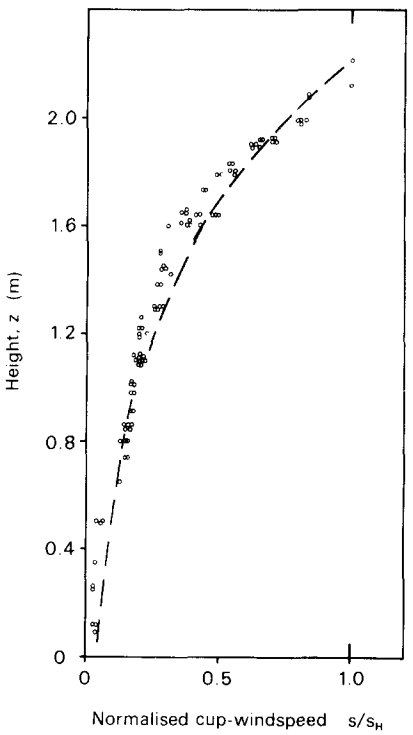

Fig. 2. Profile of normalised cup-windpseed.

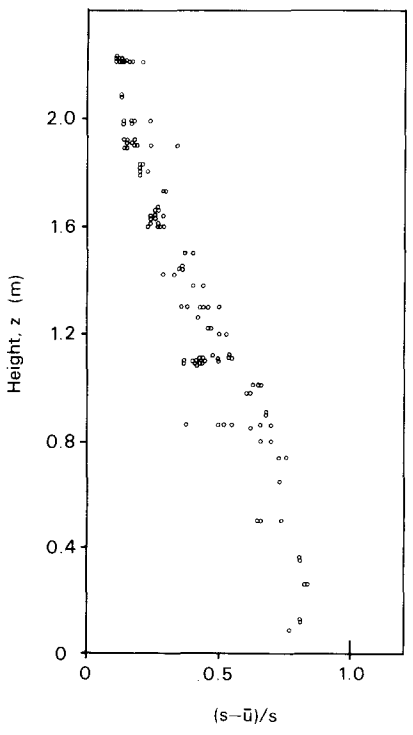

Fig. 3. Profile of proportional difference between s and $\bar{u}$.

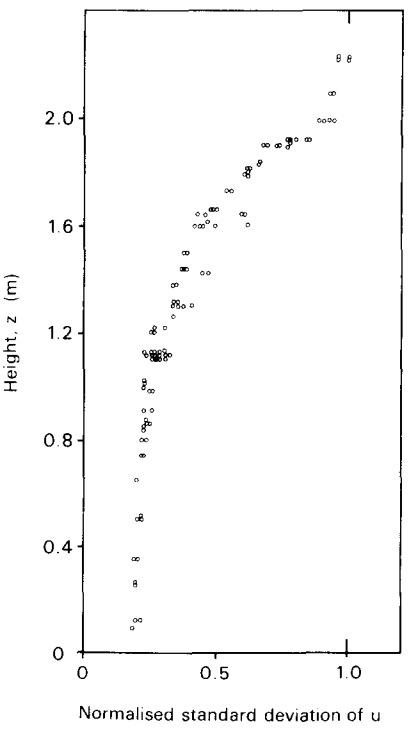

Fig. 4. Profile of normalised standard deviation of u.

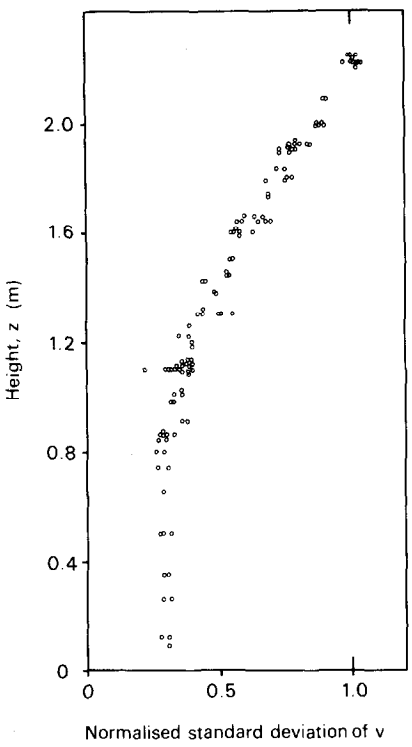

Fig. 5. Profile of normalised standard deviation of v.

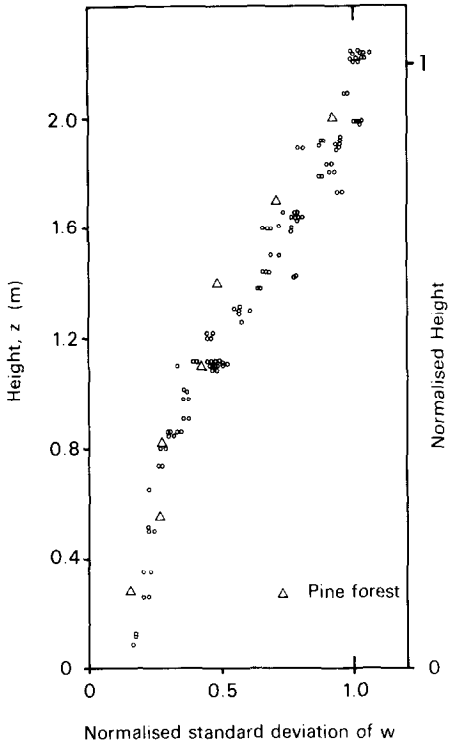

Fig. 6. Profile of normalised standard deviation of w.

Figure 3 shows that the variation with height of $(s - \bar{u})/s$ is quite regular, with increasing proportional difference between s and $\bar{u}$ as depth into the canopy increases.

Figures 4, 5, and 6 show the normalised profiles of the standard deviation of the velocity components, σ_u/σ_{uH}, σ_v/σ_{vH}, σ_w/σ_{wH}, all of which are well behaved functions of height. It is of interest that below about 70 cm the normalised standard deviations of u and v show little decrease as the surface is approached.

Figures 7, 8, and 9 show the turbulence intensity of the three velocity components versus height, $\sigma_u(z)/\bar{u}(z)$, $\sigma_v(z)/\bar{u}(z)$, and $\sigma_w(z)/\bar{u}(z)$. Above about 100 cm, the turbulence intensity is a well behaved function of height while below 100 cm, there is considerable scatter. The mean and sample standard deviation (in brackets) for 233 runs at canopy top were, for u, v, w respectively, 0.66 (0.04), 0.60 (0.05), and 0.35 (0.02). The limited data low in the canopy indicate a maximum value of the turbulence intensities at around 25 cm. Figure 10 gives the measured values of $\sigma_w(z)/s(z)$. This ratio is a more well behaved function of height than is $\sigma_w(z)/\bar{u}(z)$, suggesting that use of turbulence intensities defined with the cup windspeed would be more useful in canopy studies.

Figure 11 shows the ratio σ_v/σ_u as a function of height. At the canopy top the mean and sample standard deviation from all data were 0.82 (0.08). An increase with decreasing height can be seen, in spite of the scatter. The ratio σ_w/σ_u, shown in Figure 12, displays less scatter than σ_v/σ_u and a very definite peak at about 130 cm. The mean

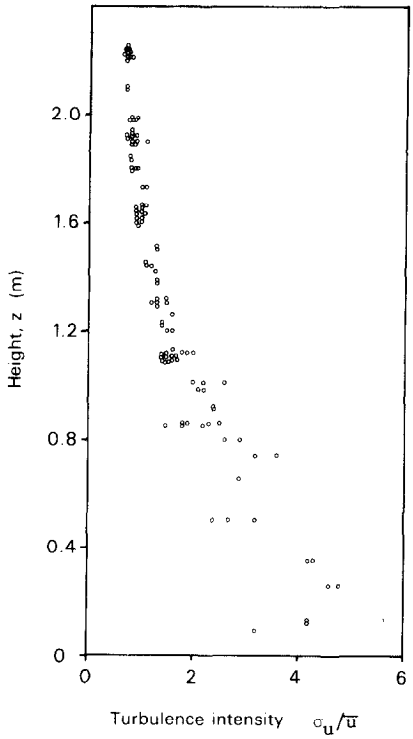

Fig. 7. Profile of turbulence intensity of *u*-component.

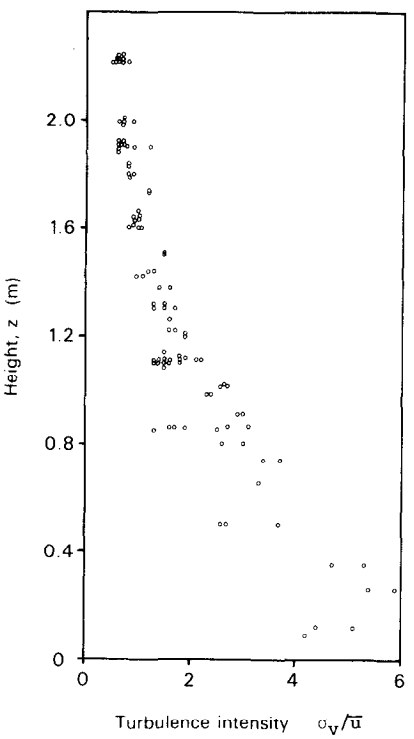

Fig. 8. Profile of turbulence intensity of *v*-component.

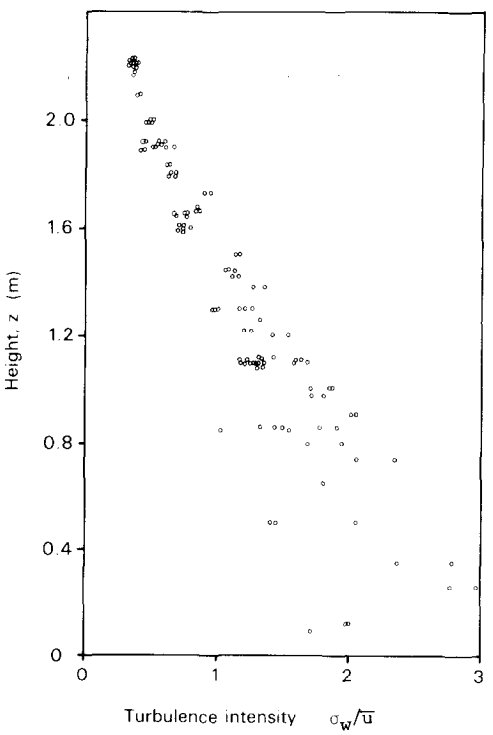

Fig. 9. Profile of turbulence intensity of *w*-component.

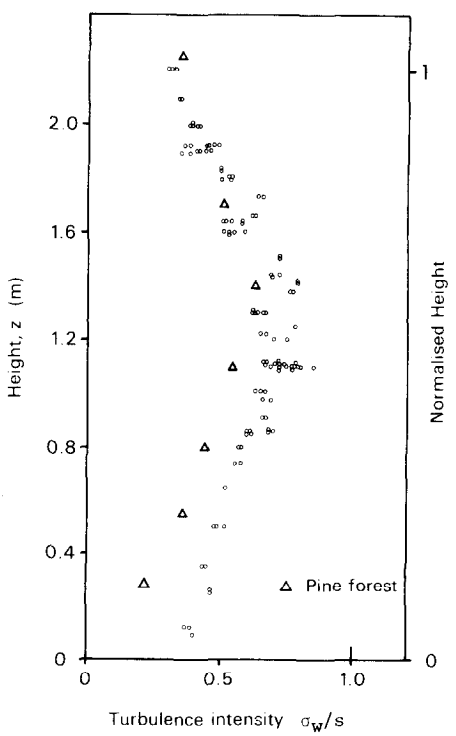

Fig. 10. Profile of turbulence intensity of *w*-component, using cup-windspeed. (Δ, data of Bradley *et al.* for pine forest).

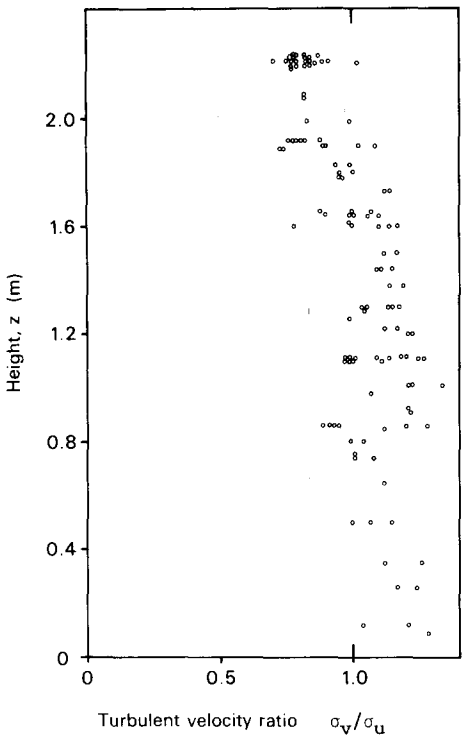

Fig. 11. Profile of ratio of standard deviations.

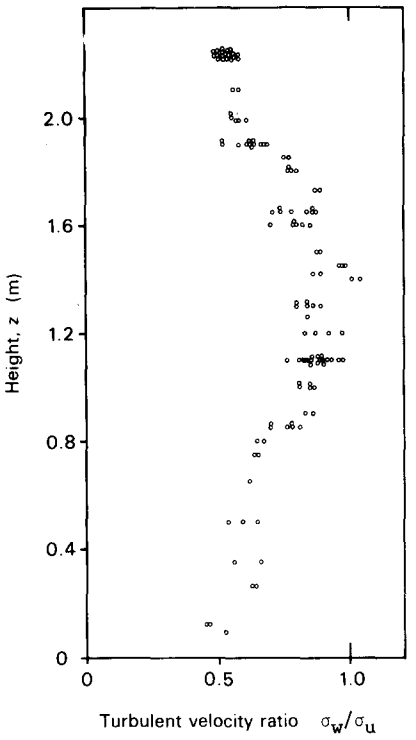

Fig. 12. Profile of ratio of standard deviations.

and sample standard deviation at the top of the canopy were 0.54 (0.03). Whereas Shaw *et al.* (1974b) found $\sigma_u > \sigma_v > \sigma_w$ at all heights in a nature corn canopy, such a general rule is not confirmed by Figures 11 and 12.

Bradley, Denmead, and Thurtell (personal communication) have made turbulence measurements in a forest of ponderosa pines in Australia. The canopy height was 16 m, with the live needles concentrated between this height and 8 m. It is of interest that their profile of σ_w/σ_{wH} is very similar to that obtained for the corn canopy (see Figure 6) when the ratios are plotted against normalised height, z/H. By the same height-normalisation it was found that their profile of σ_w/s is very similar in shape to that for the corn canopy (see Figure 10) with a peak at 1/2 the canopy height.

3.3. The Profile of Momentum Flux

The accuracy of eddy-correlation measurements of the momentum flux $\tau = -\rho\,\overline{uw}$ depends very critically on accurate orthogonality of the x and z measurement axes, precise alignment with respect to the ground plane, and absence of any false correlation introduced, for example, by the electronic circuitry. Kaimal and Haugen (1969) state that an accuracy of at least $\pm 0.1°$ in internal alignment and mounting is necessary. The split-film anemometer determines u and w from measurements of $\sqrt{(u^2 + w^2)}$, the instantaneous elevation angle $\varnothing_s$ measured with respect to the plane of the split between the two films (see Figure 1 of Shaw *et al.*, 1973), and the previously determined

alignment error $\varnothing_e$ between the plane of the splits and the plane defined by the vertical axis of the sensor. The alignment error was known to an accuracy of perhaps $\pm 0.5°$ (certainly $\pm 1°$), so that our decomposition of the wind vector into horizontal and vertical components could add of the order of 2% of the horizontal velocity to the vertical velocity. However this (pure tilt) effect is removed by the coordinate rotation performed at the end of the experimental run.

On seven days during the measurement period, close agreement was obtained between estimates of τ with two anemometers together at $z = H$ (we were unable to determine the cause of the poor agreement on other occasions). Figure 13 shows the normalised profile of momentum flux formed from the measurements on those 7 days. The scatter is not excessive. The points below $z = 60$ cm were all measured on the same (very windy) day.

In the absence of any horizontal inhomogeneity (negligible pressure gradient and acceleration) one may attribute the vertical divergence of the momentum flux to the mean drag $\overline{D}_x$ of the vegetation, which may be parameterised as

$$\overline{D}_x = \rho c_D a(z) s^2, \tag{1}$$

where $a(z)$ is the vegetative area per unit volume.

Strictly, one should write the instantaneous drag as $D_x(t) = \rho c_D(z, \mathbf{V}, t) a(z) V_x^2$ where $V_x = u\sqrt{u^2 + v^2 + w^2}$ is the projection of $\mathbf{V} \cdot \mathbf{V} = u^2 + v^2 + w^2$ on the x-axis. The drag

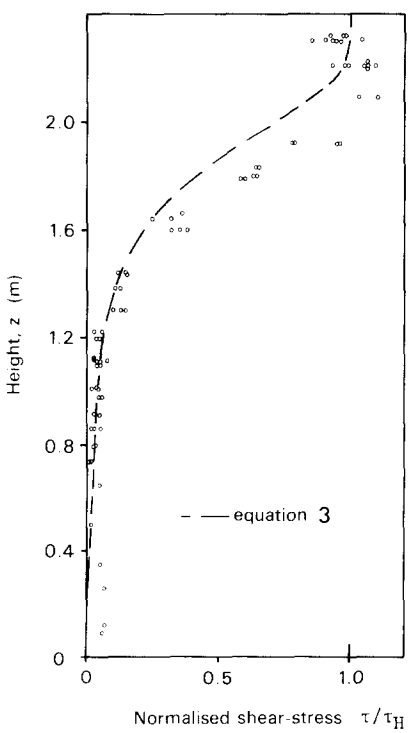

Fig. 13. Profile of normalised shear stress.

coefficient c_D may vary in response to factors such as angle of attack, leaf fluttering, the nature of the element wake (turbulent/laminar), and wake interactions (see Raupach and Thom, 1981). As this leads to excessive complication, however, and because it was found that the height-variation of $\overline{V}_x(z)/\overline{V}_x(H)$ is very similar to that of the normalised cup windspeed $s/s(H)$, there is little point in adopting the more general formulation. Accepting equation (1) and assuming that neglible momentum is transferred directly to the soil ($\tau(0) = 0$), it follows that

$$\tau(z) = \rho c_D \int_0^z a(z)s^2(z)\,\mathrm{d}z \tag{2}$$

and

$$\frac{\tau(z)}{\tau(H)} = \int_0^z a(z)(s/s_H)^2\,\mathrm{d}z \Big/ \int_0^H a(z)(s/s_H)^2\,\mathrm{d}z. \tag{3}$$

In order to calculate a profile of normalised momentum flux, $a(z)$ was determined from a sample of 18 plants collected on 3 different days, between which no large differences were found. For each of 7 layers, $a(z)$ was calculated by defining the total surface area of plant tissue to be the sum of

(i) twice the 1-sided planar leaf area

(ii) the cylindrical area of stem and ears

(iii) the area of a cylinder of average tassle diameter and length equal to total length of tassle

and normalising by the relevant canopy volume involved. Table II shows the height-dependence of $a(z)$.

The 'total area index', the total surface area per unit ground area, was

$$\int_0^H a(z)\,\mathrm{d}z = 7.0,$$

TABLE II

The height-distribution of vegetative area within the canopy. The ground area occupied by one plant is 1695 cm^2, (59000 plants/ha).

Height interval	Planar 1-sided leaf area (cm^2) per plant	Total area (cm^2) per plant	$a(z)$ (cm^{-1})
0– 33	127	551	0.99×10^{-2}
34– 66	477	1212	2.17×10^{-2}
67–100	810	2201	3.93×10^{-2}
101–133	990	2417	4.32×10^{-2}
134–166	1247	2619	4.68×10^{-2}
167–200	1126	2434	4.35×10^{-2}
201–233	113	441	0.79×10^{-2}
0–233	4890	11875	

and the conventional leaf area index, which includes only the 1-sided planar leaf area, was 2.9.

The profile of normalised momentum flux according to Equation (3) is plotted on Figure 13 with the observations. Although a drag coefficient which decreases with increasing height would give a closer fit to the observations (i.e., a deeper penetration of the momentum flux), a constant drag coefficient is a good first approximation.

From Equation (2) it follows that

$$\tau_H = \rho c_D s_H^2 \int_0^H a(z)(s/s_H)^2 \, dz.$$

The value of the integral was calculated to be 0.84. For periods during which both anemometers were together at $z = H$, the estimates from the two anemometers were averaged to obtain 24 combined estimates of (τ_H, s_H^2) with s_H in the range $1.36 \text{ m s}^{-1} < s_H < 3.10 \text{ m s}^{-1}$. These data are shown on Figure 14. From the slope of the observed relationship, it follows that $C_D \sim 0.07$. For comparison with data obtained using $a(z)$ = 1-sided area, this value must be multiplied by 11875/4890 (see Table II) which gives $C_D = 0.17$. Values from 0.13 to 0.30 for the drag coefficient of a single corn leaf in a wind tunnel were reported by den Hartog (1973), depending on angle of attack, windspeed and leaf size. A smaller value of the drag coefficient for the whole canopy is expected as a result of aerodynamic interference between leaves (Thom, 1971; Hoerner, 1965).

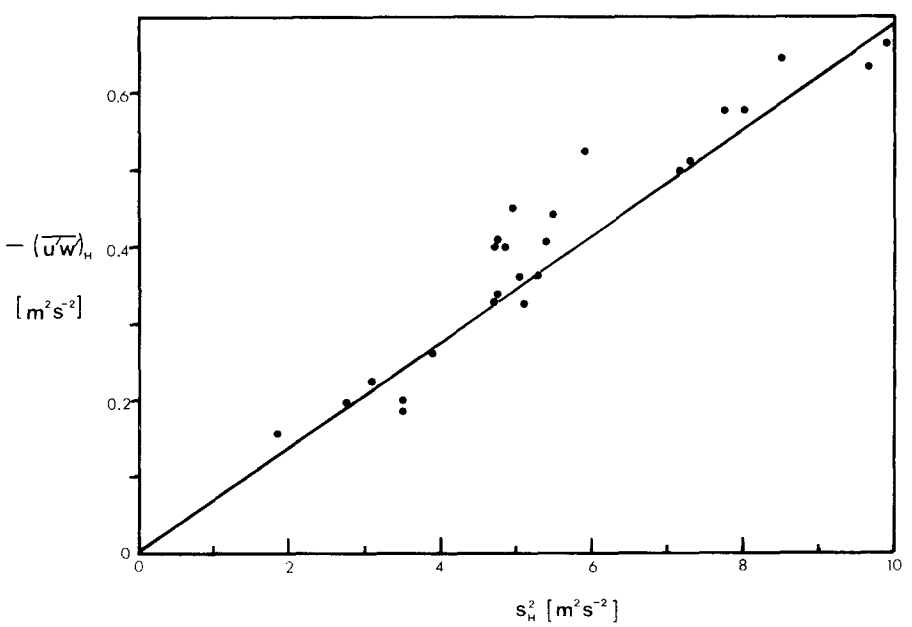

Fig. 14. Shear stress as a function of windspeed at $z = H$. The line is a least squares fit.

3.4. PROFILE OF EDDY HEAT FLUX

On 8 days during 1977, eddy heat fluxes were measured at the top of and within the canopy. The profile of normalised eddy heat flux is shown in Figure 15. The data are for periods when $A_H > 25$ W m^{-2}, and include a wide range of values of A_H and net radiation at canopy height, R_H. The spread of the points about a value of unity when both measurements are made at H indicates the degree of uncertainty. The variability both from day to day and from $\frac{1}{2}$ hr to $\frac{1}{2}$ hr is considerable, though at 160 cm, where the scatter is greatest, the variability from day to day exceeds that within each day. The greater variability in the shape of the heat flux profile than in the momentum flux profile is a reflection of the fact that the drag is (for a given canopy) a function of only a single

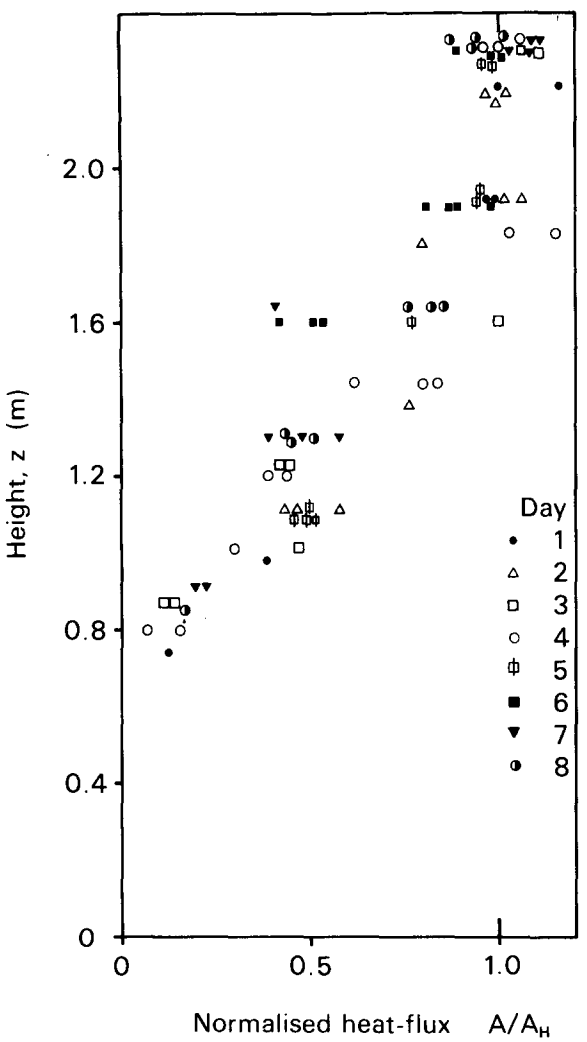

Fig. 15. Daily profiles of normalised sensible heat flux density. The day numbers are identified in Table III.

TABLE III

Values of measured variables possibly affecting the ratio of heat fluxes, $A(160)/A_H$.

Day number (Figure 15)	7	6	5	8	3	Correlation
Day/Month	28/8	26/8	24/8	3/9	12/8	coefficient
$A(160)/A_H$	0.41	0.52	0.76	0.84	1.0	
Time (EDT)	1225–1255	1515–1545	1515–1545	1315–1345	1215–1245	
$\overline{u}_H$ (cm s^{-1})	243	141	255	158	178	−0.22
R_H (W m^{-2})	340	434	465	525	488	0.86
A_H (W m^{-2})	46	50	106	196	99	0.66
σ_{w_H} (cm s^{-1})	85	50	89	65	58	−0.24
σ_{T_H} (°C)	0.28	0.26	0.31	0.86	0.69	0.77
Absolute humidity (g m^{-3})	18	9	8	10	8	
Air temperature (°C)	28	22	17	20	20	
Sky conditions	4/10 Cu	4/10 Ci	Clear	3/10 Cu	6/10 Cu	

'external' parameter, which may be chosen as the cup windspeed at canopy height, while the source strength for sensible heat at any height in the canopy depends in a complex fashion on the radiation conditions, moisture availability and physiology of the plants.

Although there are insufficient data to determine the factors controlling the profile shape, the wide spread from day to day in $A(160)/A_H$ provides an opportunity to look for qualitatively important factors. Table III compares the values of possibly relevant parameters; the parameter most closely correlated with $A(160)/A_H$ is R_H. Correlation coefficients were obtained by a least-square fit.

In agreement with the findings of Shaw *et al.* (1974a), no systematic variation in $A(z)/A_H$ with solar elevation was inferred. On 24 August 1977, the sky was clear from 1500 EDT onwards. Four consecutive half-hourly values of $A(110)/A(230)$ between 1600 EDT and 1800 EDT were 0.49, 0.49, 0.46, 0.51 (with $A(230)$ = 86, 74, 50, 38 W m^{-2}). Between 1800 and 1830, $A(110)/A(230)$ = 0.62, though over this period $A(230)$ = 23 W m^{-2}. From these measurements (the only suitable clear-sky period), it seems that solar elevation need not have a large effect on the shape of $A(z)/A_H$.

In the upper $\simeq$ 50 cm of the canopy, there is little divergence of the sensible heat flux density. In the layer 180–80 cm, the divergence is quite variable from day to day, with the average pattern appearing to be a constant divergence across the layer (constant source strength).

4. Data of 1976 – Time Series Analysis

4.1. Length and Time Scales

In many models of turbulent energy, momentum, and mass exchange, the concept of a 'length scale' arises, either directly or indirectly measurable, and interpreted broadly speaking as a measure of the local eddy size, or the distance over which exchange is occurring. Examples are:

(i) the Prandtl mixing length

$$l = \sqrt{\tau/\rho} \Big/ \frac{\mathrm{d}\bar{u}}{\mathrm{d}z},$$

a gradient-diffusion type length scale used to relate shear stress to the mean velocity shear (first-order closure) and observed to have the value kz (k = von Karman's constant $\approx$ 0.4) in the constant stress layer in flow above a flat surface.

(ii) Taylor's Lagrangian length scale

$$\mathscr{L}_{\mathrm{L}} = \int_0^\infty \overline{w_L(t) w_L(t+\xi)}\, \mathrm{d}\xi/\sigma_w^2,$$

where w_{L} is the vertical velocity of a tagged fluid element. Taylor (1921) showed that this length scale is precisely related to the rate of spread of a puff of marked fluid elements in a turbulent flow. An estimate of this length scale is a required input to the

trajectory-simulation model of turbulent dispersion in a plant canopy described by Wilson *et al.* (1981). As Lagrangian measurements near ground are very difficult, $\mathscr{L}_L$ is often estimated from a knowledge of the Eulerian time scale

$$\Gamma_E = \int_0^\infty R_E(\xi)\, d\xi$$

where $R_E(\xi)$ is the Eulerian autocorrelation function

$$R_E(\xi) = \overline{w(t)\, w(t + \xi)}/\sigma_w^2$$

defined from measurements of w at a point fixed in space.

(iii) The wide variety of length scales defined in higher-order closure relations now being employed in numerical models of turbulent flows. For example, the higher-order closure model for canopy flow described by Wilson and Shaw (1977) uses three height-dependent length scales all chosen as multiples of l', which for a corn canopy was chosen as l' = the smaller of $(kz, 0.3/a(z))$ with $k = 0.4$ and $a(z)$ = leaf area density. In the bottom of the canopy $a(z)$ is small, so that l' is the conventional Prandtl length scale for flow in a constant stress layer.

It is important that a clear idea of the height – dependence of the eddy size or exchange depth be obtained, preferably by direct measurement.

Uchijima and Wright (1964) derived values of the Prandtl mixing-length from measurements of the wind profile using heated thermocouple anemometers in and above a corn canopy of height $H \simeq 140$ cm. The local stress $\tau(z)$ was determined from the wind profile and the leaf area per unit volume using the arguments given in Section (3.3) herein. Their Figure 6 shows $l(z) \simeq 0.4z$ in the lower half of the canopy (with estimates at 20 and 40 cm, which are apparently below the lowest anemometer (50 cm) and whose origin is therefore hard to understand). Maximum values of l occurred in mid-canopy, with reduced values near the top of the canopy, which are more consistent with $l \simeq 0.4$ $(z\text{-}d)$, where d is the displacement height measured from the wind profile above the crop. However, note that the information here arises from the mean wind profily alone. Bearing in mind the small speeds and stresses measured deep in the Elora canopy, one cannot expect this procedure to be very accurate.

The split-film anemometer data recorded on magnetic tape enabled calculation of an Eulerian time scale in and above the corn canopy. The recorded data were reproduced and autocovariance functions computed for the u, v, and w components using the techniques described by Silverside (1972). Prior to the calculation of the autocovariance functions, the data were digitally filtered into three overlapping bands whose combined frequency range was 0.003 Hz to 20 Hz. Three autocovariance functions were computed for each orthogonal component, one for each frequency band. Each was defined for 50 lags, the lags being 10.0, 0.5, 0.025 s duration for the low, medium and high frequency bands, respectively.

For 14 different periods ranging in length from 1 to 4 hr, estimates of the Eulerian time scales for the u and w components were calculated from the integral of the

TABLE IV

Length and time scales*

Height (cm)	$\bar{u}$ (cm s^{-1})	$\overline{w'^2}$ (cm^2 s^{-2})	$R_{uu}(0)$ (cm^2 s^{-2})	$R_{ww}(0)$ (cm^2 s^{-2})	$\int R_{uu}$ (cm^2 s^{-1})	$\int R_{ww}$ (cm^2 s^{-1})	Γ_u (s)	Γ_w (s)	Γ'_w (s)	$\Gamma_w \sigma_w$ (cm)	$\Gamma_w \bar{u}$ (cm)
655	233	2626	6928	2453	63452	2981	9.16	1.22	0.776	62.5	290
655	313	3085	8817	2900	36422	2570	4.13	0.866	0.714	48.1	271
370	296	4289	12640	4031	48358	1763	3.83	0.437	0.445	28.6	129
370	229	2401	9416	2303	44499	1265	4.73	0.549	0.415	26.9	121
370	442	9109	30340	8794	52258	2402	1.72	0.285	0.433	27.2	126
370	435	8421	29100	8535	55249	2580	1.90	0.302	0.451	27.7	131
370	257	3353	9403	3205	31465	2084	3.35	0.650	0.574	37.6	167
275	174	2332	6421	2197	17826	1347	2.78	0.613	0.390	29.6	107
225	119	1613	6073	1494	16566	839	2.73	0.562	0.355	22.6	66.9
225	200	3971	14690	3246	26789	1059	1.82	0.326	0.325	20.5	65.2
175	127	3195	8547	3166	11541	1230	1.35	0.389	0.422	22.0	49.4
175	124	2726	8134	2662	12450	1035	1.53	0.389	0.397	20.3	48.2
125	68.6	2797	5523	2768	3860	598	0.666	0.216	0.387	11.4	14.8
75	27.5	708	1785	655	1069	280	0.599	0.427	0.657	11.4	11.7

* Length and time scales. $R_{ww}(0)$ was computed from the recorded and subsequently filtered data. The filtering removes energy at both low and high frequencies and therefore $\overline{w'^2}$ exceeds $R_{ww}(0)$.

autocovariance function using

$$\Gamma_\alpha = \frac{1}{R_{\alpha\alpha}(0)} \int_0^\beta R_{\alpha\alpha}(t)\, dt$$

where

Γ_α = Eulerian time scale of u or w component.

$R_{\alpha\alpha}(t)$ = autocovariance at lag t.*

β = smallest time at which $R_{\alpha\alpha}(t)$ becomes negative.

A summary of the autocovariance integrals and time scales for each of the selected 14 periods is given in Table IV.

The time scale for any particular run is a function of the mean speed at that height since the length scale at each height remains constant (in principle). Therefore, for graphical presentation of time-scale data obtained from different runs and different days, the data had to be normalized to an 'average' day. This was done using the relationship:

$$\Gamma'_w = \Gamma_w \frac{u_{370}}{\bar{u}_{370}}$$

where

Γ'_w = normalized time scale of the vertical turbulence

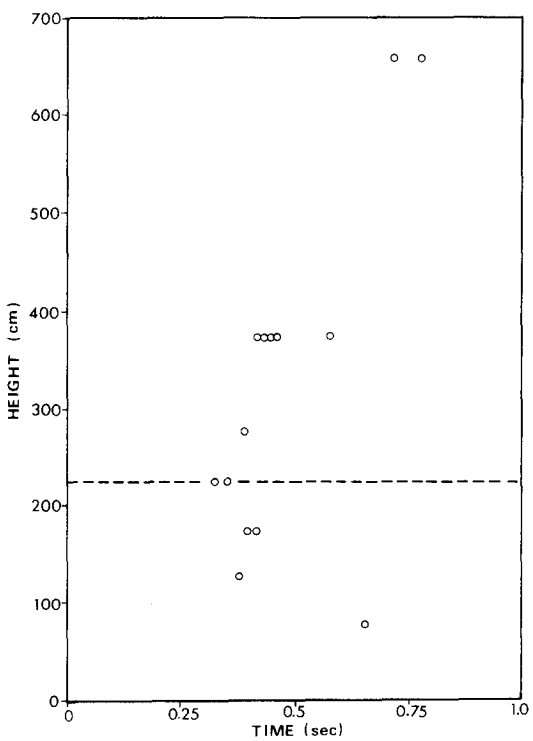

Fig. 16. Profile of Eulerian timescale Γ'_w. Each point represents one run. The dashed line is the top of the canopy.

* R henceforth denotes the autocovariance function rather than the dimensionless autocorrelation function.

Γ_w = the observed time scale of the vertical turbulence
u_{370} = the mean wind speed at 370 cm over the period when Γ_w was calculated
$\bar{u}_{370}$ = the average wind speed at 370 cm over all runs and all days.

A profile of the normalized time scale, Γ'_w, is shown in Figure 16. The value of $\bar{u}_{370}$ for the 'average' day was 291 cm s^{-1}. As shown in the figure, the time scale had a minimum at the top of the canopy, although without the single measurement at 75 cm, this would be in doubt. However, the concept of high-velocity low-persistence motion in the dense upper canopy (where most of the momentum is absorbed) and low-velocity longer-persistence wafting in the more open lower canopy seems plausible.

Two length scales were formed from Γ_w,

$$L_w = \Gamma_w \sigma_w$$

$$L_u = \Gamma_w \bar{u}.$$

Figure 17 shows the height dependence of these length scales. Although there is insufficient data to be conclusive, it appears that

$$L_w \simeq 0.1z$$

$$L_u \simeq 0.5(z - 75 \text{ cm}).$$

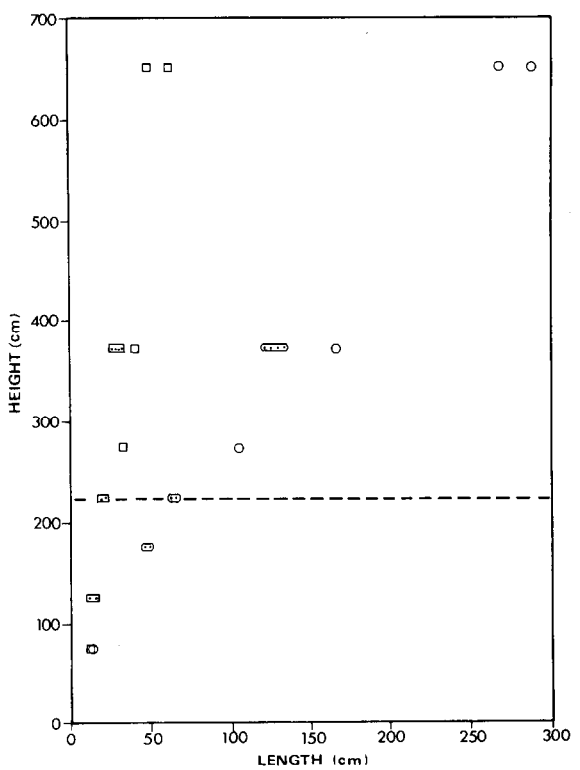

Fig. 17. Profiles of Eulerian length scales L_u(⊙) and L_w(□). Each point represents one run. The dashed line is the top of the canopy.

Seginer *et al.* (1976) measured (directly) the Prandtl mixing-length l and the Eulerian length scales $L_{u,v,w} = \Gamma_{u,v,w}\bar{u}$ within and above an array of cylindrical rods in a wind tunnel. While the 3 Eulerian length scales all increased with height in the canopy, l was approximately constant (except very near ground), the latter being consistent with their measurement of an exponential wind profile which did not show the reversal of curvature near canopy top often seen in corn canopy wind profiles. This finding highlights the large difference in magnitude between very different types of length scales. Although still well-defined, these length-scales are harder to interpret in a canopy where both the constituent velocity and times scales vary, than in the atmospheric layer well above the canopy, in which the velocity scale is approximately constant and the interpretation of $\sigma_w\Gamma$ or $\bar{u}\Gamma$ as a characteristic eddy size seems quite reasonable.

At this time it is not possible to generalise with any certainty as to the behaviour of L_w, L_u with height in a crop canopy. A great deal of effort is involved in a single measurement of L_u, L_w and it is likely to be a long time before definitive profiles have been obtained for a variety of types of canopy. However, it should be stressed that it is worthwhile to know these statistics; for example, they are prerequisities to successful simulation of disease spore or pollen trajectories in a crop.

4.2. Spectral characteristics

Power spectra of the u, v and w velocity components were computed for 7 different periods ranging in length from 1 to 4 hr with one set of spectra computed at each of 7 levels. The data were sampled at 160 Hz and the spectra computed in 3 overlapping bands ranging in frequency from 0.001 to 20 Hz. The individual spectra were non-dimensionalized and spectra from each height compared.

A non-dimensional frequency f was defined by $f = 2\pi nz/\bar{u}$ where
n = the observed frequency
z = the instrument height
$\bar{u}$ = the mean wind speed at height z.

As discussed by Silversides *et al.* (1974), this non-dimensionalizing scheme assumes that the length scale of the turbulence is a linear function of height and that the length-scale goes to zero at the surface. Based on the information in Figure 17, the length L_w appears to meet this criterion. A second assumption is that Taylor's hypothesis can be applied in order to convert measurements from the time domain to the space domain. The frozen-turbulence approximation is probably inaccurate in the highly turbulent regions of the lower canopy.

A non-dimensional spectral density $S(f)$ was defined by

$$S(f) = \frac{G_\alpha(f)}{\sigma^2}\,\frac{\bar{u}}{z}$$

where
$G_\alpha(f)$ = the observed spectral density
α = u, v, or w
σ^2 = the variance of u, v, or w at height z and for f below 20 Hz.

No corrections were made for stability.

Figure 18a, b, c presents the non-dimensionalized power spectra of the u, v, and w components respectively for data from 4 different heights above the canopy. The heights are indicated in the figures. All spectra have $-5/3$ regions spanning at least 2 decades of frequency. The upper level u and v spectra (370 and 655 cm) have slightly smaller values at higher frequencies than those from the lower 2 levels. This is because the spectra were normalized by the total variance. The upper levels have significantly more variance at the extremely low frequencies ($f < 0.005$) and therefore the non-dimensionalized variance at the higher frequencies is reduced. The w spectra match well at all frequencies.

Kaimal *et al.* (1972) gave empirical formulae (their equations 21) which summarise the velocity spectra measured in the Kansas surface-layer experiments. On each of Figures 18a, b, c, several spectral-density values from the Kansas formulae are plotted (assuming $\sigma_u = 2.30u_*$, $\sigma_v = 1.7u_*$, and $\sigma_w = 1.25u_*$). The above-canopy Elora spectra of u and w in particular differ negligibly from the neutral Kansas spectra.

The power spectra of the u, v, and w components observed at various depths within the canopy are presented in Figure 19a, b, c, respectively. As with the observations above the canopy, there is an extensive $-5/3$ region spanning at least 2 decades of frequency at all depths within the canopy. The w-spectra from different heights match acceptably-well using the present scaling scheme, in contrast to the findings of Shaw *et al.* (1974a). Some improvement in the normalisation of the u- and v-spectra could be obtained by writing the non-dimensionalising length scale as z-z_1, where z_1 is an arbitrary displacement length. In view of the uncertainty in our knowledge and interpretation of canopy length scales, such a procedure would at this stage be pointless.

5. Conclusion

The vertical profiles of horizontal windspeed $s(z)$ and $\bar{u}(z)$, the standard deviations $\sigma_u(z)$, $\sigma_v(z)$, $\sigma_w(z)$, and the momentum flux $\tau(z)$ may be normalised by their canopy-top values to obtain profiles whose shape varies little from day to day, implying that stability effects were not very important within the canopy during the periods when the measurements were obtained. The flow within the canopy may therefore be characterised by a single windspeed, for example the canopy-top cup windspeed s_H. However it must be pointed out that these measurements have necessarily been made on days sufficiently windy for the split-film anemometers to operate satisfactorily, and it is suspected that the canopy flow statistics would be very different under calm conditions with high net radiation.

The shape of the profile of normalised sensible heat flux changes very significantly from day to day; of the variables measured, the sensible heat flux most closely paralleled the value of the net radiation at the top of the canopy. The assumption of a constant drag coefficient leads to a slightly shallower predicted penetration of the momentum flux into the canopy than was observed, implying that the drag coefficient decreases with increasing height. The mean canopy drag coefficient was found to be 0.17.

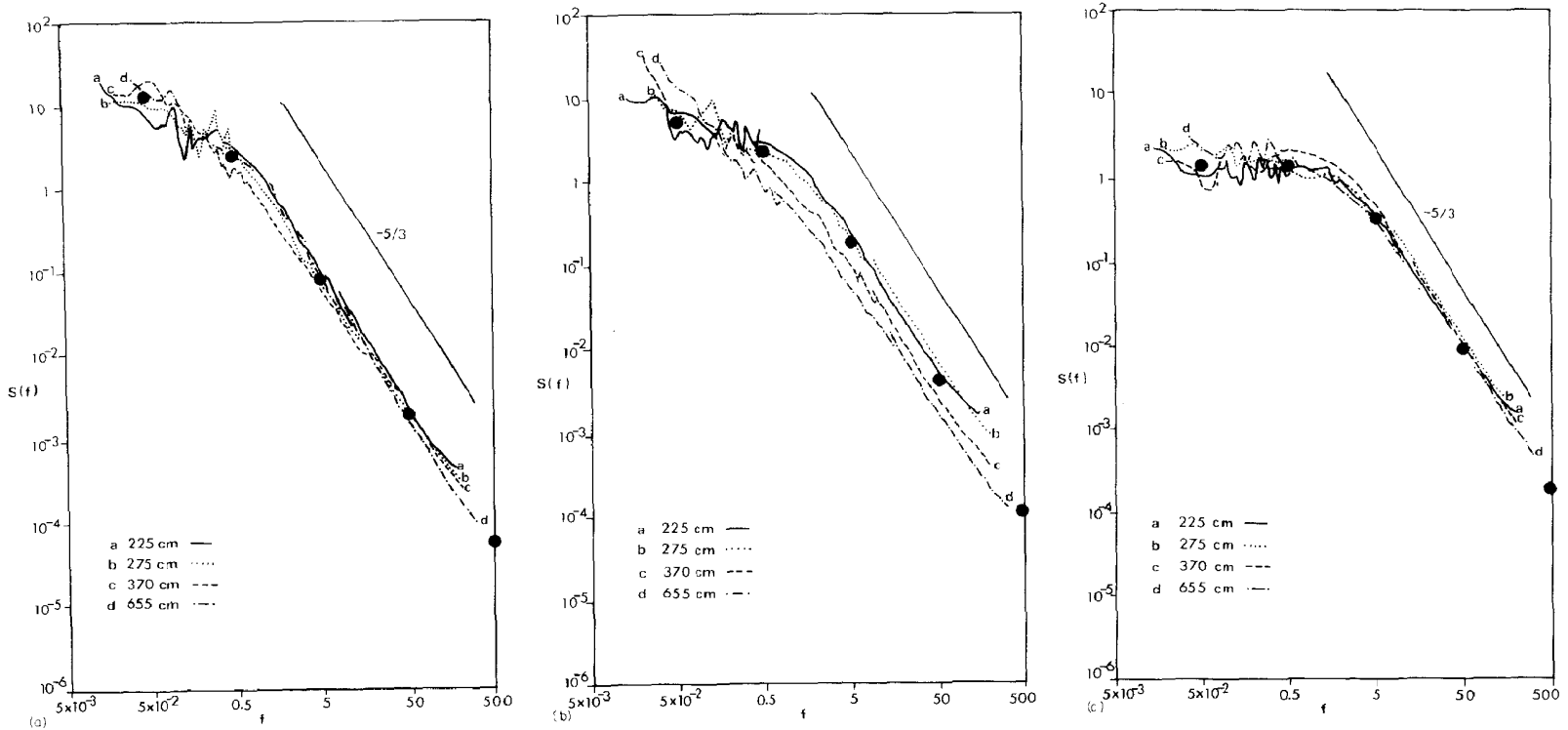

Fig. 18. Comparison of normalised spectra S_{uu} (a); S_{vv} (b); and S_{ww} (c) at four different heights above the canopy. The solid points are calculated from formulae given by Kaimal *et al.* (1972) which summarise the surface-layer spectra measured in the Kansas experiments.

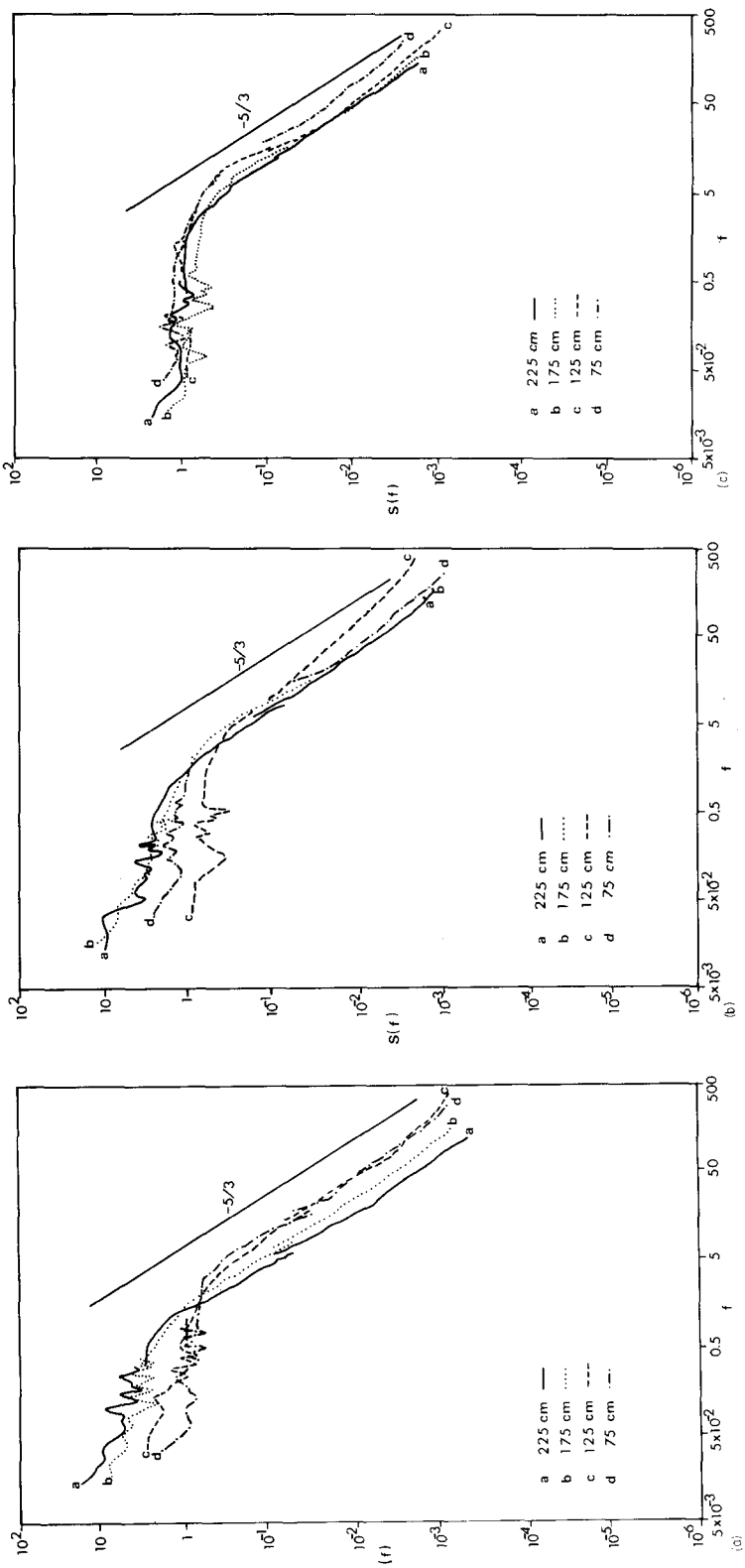

Fig. 19. *Comparison of normalised spectra* S_{uu} (a); S_{vv} (b); and S_{ww} (c) at four different heights within the canopy.

The estimated vertical profile of the Eulerian time scale of the turbulence for an average day shows a local minimum in the timescale at the top of the canopy. The length scale formed as the product of observed timescale and root-mean-square vertical velocity appears to fit the expression $L_w \simeq 0.1z$, while the length scale formed using the horizontal windspeed is given approximately by 0.5 ($z - 75$ cm).

All power spectra presented for each of the three velocity components had extensive $-5/3$ regions spanning at least 2 decades of frequency. The span of the $-5/3$ region appeared to increase with increasing height above the soil surface. In the lowest regions of the canopy, the nondimensionalizing parameter $z/\bar{u}$ was adequate for the w spectra but not for the u and v data.

References

Bill, R. G., Allen, L. H., Anderson, T., Gebhart, B., and Lemon, E.: 1976, 'Turbulent Transport within and Above a Maize Canopy', *Boundary-Layer Meteorol.* **10**, 199–220.

Corrsin, S.: 1974, 'Limitations of Gradient Transport Models in Random Walks and in Turbulence', *Adv. Geophys.* **18A**, 25–60.

den Hartog, G.: 1973, 'A Field Study of the Turbulent Transport of Momentum between the Atmosphere and a Vegetative Canopy', Ph.D. dissertation, Univ. of Guelph, Guelph, Ontario, Canada.

Hoerner, S. F.: 1965, *Fluid Dynamic Drag*, published by S. F. Hoerner. Library of Congress Catalog Card Number 64-19666.

Kaimal, J. C. and Haugen, D. A.: 1969, 'Some Errors in the Measurement of Reynolds Stress', *J. Appl. Meteorol.* **8**, 460–462.

Kaimal, J. C., Wyngaard, J. C., Izumi, Y., and Coté, O. R.: 1972, 'Spectral Characteristics of Surface-layer Turbulence', *Quart. J. Roy. Meteorol. Soc.* **98**, 563.

Lang, A. R. G. and Leuning, R.: 1981, 'New Omnidirectional Anemometer with no Moving Parts', *Boundary Layer Meteorol.* **20**, 445–457.

Raupach, M. R. and Thom, A. S.: 1981, 'Turbulence in and above Plant Canopies', *Ann. Rev. Fluid Mech.* **13**, 97–129.

Seginer, I., Mulhearn, P. J., Bradley, E. F., and Finnigan, J. J.: 1976, 'Turbulent Flow in a Model Plant Canopy', *Boundary-Layer Meteorol.* **10**, 423–453.

Shaw, R. H., Kidd, G., and Thurtell, G. W.: 1973, 'A Miniature Three-Dimensional Anemometer for Use within and above Plant Canopies', *Boundary-Layer Meteorol.* **3**, 359–380.

Shaw, R. H., Silversides, R. H., and Thurtell, G. W.: 1974a, 'Some Observations of Turbulence and Turbulent Transport Within and Above Plant Canopies', *Boundary-Layer Meteorol.* **5**, 429–449.

Shaw, R. H., den Hartog, C., King, K. M., and Thurtell, G. W.: 1974b, 'Measurements of Mean Wind Flow and Three-Dimensional Turbulence Intensity within a Mature Corn Canopy', *Agric. Meteorol.* **13**, 419–425.

Silversides, R. H.: 1972, 'The Structure of Thermal Turbulence Above and Within Caponies of Zea Mays (L) and Pinus Resinosa (AIT)', Ph.D. Thesis, University of Guelph, Guelph, Ontario, Canada.

Silversides, R. H.: 1974, 'On Scaling Parameters for Turbulence Spectra Within Plant Canopies', *Agric. Meteorol.* **13**, 203–211.

Tanner, C. B. and Thurtell, G. W.: 1969, 'Anemoclinometer Measurements of Reynolds Stress and Heat Transport in the Atmospheric Surface Layer', Research and Development Technical Report, ECOM 66-G22-F, Final Report.

Taylor, G. I.: 1921, 'Diffusion by Continuous Movements', *Proc. London Math. Soc.* **20**, 196–211.

Thom, A. S.: 1971, 'Momentum Absorption by Vegetation', *Quart. J. Roy. Meteorol. Soc.* **97**, 414–428.

Uchijima, Z. and Wright, J. L.: 1964, 'An Experimental Study of Airflow in a Corn-Plant-Air Layer', *Bull. Nat. Inst. Agric. Sci. (Japan) A11.*

Ward, D. P.: 1977, 'Some Observations of Atmospheric Turbulence Within and Above a Corn Canopy Using a Modified Split Film Heat Transfer Anemometer', M.Sc. Thesis, University of Guelph, Guelph, Ontario, Canada.

Wilson, N. R. and Shaw, R. H.: 1977, 'A Higher Order Closure Model for Canopy Flow', *J. Appl. Meteorol.* **16**, 1197–1205.

Wilson, J. D., Thurtell, G. W., and Kidd, G. E.: 1981, 'Numerical Simulation of Particle Trajectories in Inhomogeneous Turbulence, II: Systems with Variable Turbulent Velocity Scale', *Boundary-Layer Meteorol.* **21**, 423–441.